ELSEVIER

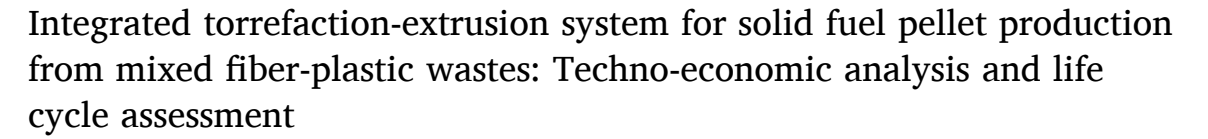
Contents lists available at ScienceDirect

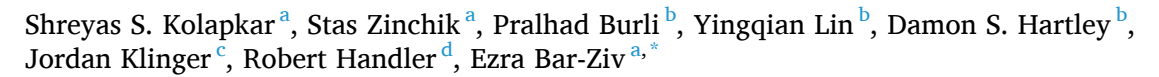
# Fuel Processing Technology

journal homepage: www.elsevier.com/locate/fuproc



# Research article





- <sup>a</sup> Dept. of Mechanical Engineering-Engineering Mechanics, Michigan Technological University, Houghton, MI 49931, USA
- <sup>b</sup> Operations Research and Analysis, Idaho National Laboratory, Idaho Falls, ID 83415, USA
- <sup>c</sup> Energy and Environment Science & Technology Directorate, Idaho National Laboratory, Idaho Falls, ID 83415, USA
- <sup>d</sup> Sustainable Futures Institute, Michigan Technological University, Houghton, MI 49931, USA

#### ARTICLE INFO

#### Keywords:

Pilot scale torrefaction-extrusion system Techno-economic analysis (TEA) Life cycle assessment (LCA)

#### ABSTRACT

The world is witnessing an unprecedented generation and accumulation of fiber-plastic wastes resulting in various challenges due to inconsistency, waste-stream heterogeneity, conveying issues, self-heating, and difficulty in pelletization. This study presents a novel pilot-scale system that integrates torrefaction and extrusion to convert mix fiber-plastic waste into fuel pellets. The produced pellets have low cost, high heating value, better uniformity, and low environmental impact. They can be used as solid fuels or as feedstock for pyrolysis and gasification. To evaluate the pellet cost and its environmental impact, we performed Techno-Economic Analysis (TEA) and Life Cycle Assessment (LCA). The TEA integrates research findings from the torrefaction-extrusion project with the techno-economic models and estimates the costs, energy consumption, and mass balances for pelletizing and torrefaction. The analysis indicates that the baseline cost of producing uniform pellets is about \$55.28/dry tonne (2020\$). LCA results indicate that the torrefied product has cradle-to-gate embodied greenhouse gas emissions that are net negative, although they are higher than a comparable forest-derived woodchip product. Fossil energy demand for the torrefied product is lower than the forest-derived chip, indicating the torrefied product has strong potential for use as an environmentally beneficial feedstock for future processing.

# 1. Introduction

As the world population continues to increase, so does waste generation. It is anticipated that, by 2050, humans will generate wastes at a record high of 3.4 billion t/yr worldwide [1]. As a result, we are witnessing an unprecedented accumulation of fiber/plastic wastes in landfills, land, and oceans with well-documented negative consequences [2,3]. To address this, some countries have adapted the waste-to-energy approach as a preferred path [4]; however, the downside of this approach is that waste-to-energy can be costly due to high operational and gas cleanup costs to meet emission standards [5]. In parallel, in the U.S., states like Florida and California have mandated the approach of high recycling rates [6,7], but with world events like the Chinese ban on recyclable imports [8], critical issues with recycling have surfaced.

Apart from these challenges, recycling cost is often driven up due to barriers like (a) inconsistencies of wastes, (b) heterogeneity in the waste stream, (c) bridging and conveying issues due to the low feedstock density, (d) inefficient separation technologies for recyclable polymers, and (e) difficulties in flowing wastes into reactors. As we strive to become truly sustainable, these challenges must be addressed.

One pathway to address these challenges is the thermo-chemical pathway of torrefaction. It is a process of heating the feedstock at temperatures usually ranging from 250 °C to 350 °C in the absence of oxygen or in an oxygen-starved environment [9,10]. Torrefaction converts the feedstock mainly into solids, which can be used as a solid fuel in cofiring boilers and cement kilns or upgraded to transportation fuels, sustainable aviation fuels, and chemicals through catalytic pyrolysis or gasification [11–14]. Torrefaction using biomass as a feedstock has been

E-mail address: ebarziv@mtu.edu (E. Bar-Ziv).



<sup>\*</sup> Corresponding author at: Department of Mechanical Engineering-Engineering Mechanics, Michigan Technological University, R.L. Smith Building, Room 1012, 1400 Townsend Dr., Houghton, MI 49931-1295, USA.

studied extensively [15–18] and has been regarded as a promising energy source [19–22]. However, biomass presents several disadvantages, as pointed by the five years long industrial-scale study by Nunes [23] and several other studies [19,24] like low feedstock density, problems associated with logistics and handling, high raw material prices, high moisture contents, self-heating, difficulty in pelletizing and excessive wear of production equipment.

The current study focuses on the torrefaction of fiber-plastic waste blends; the use of plastic along with fiber (biomass) addresses the biomass-related issues mentioned above in Nunes's study [23]. It has been discovered that plastic acts as an enabler to the torrefaction-extrusion process by providing higher calorific value [25], significantly reducing self-heating tendency by encapsulation of reactive torrefied fiber [26], acting as a lubricant to reduce the wear and tear of the production equipment, facilitating material binding during the extrusion-pelletization processes and also making produced pellets water repellant [25]. Along with biomass, torrefaction of fiber-plastic wastes has also been extensively studied and documented [10,25,27,28].

The torrefaction technology presented in the current study is an integrated torrefaction-extrusion technology that can produce torrefied pellets from a mix of fiber and plastic wastes. Both paddles and the extruder have been extensively studied independently; for instance, Bar-Ziv et al. studied the use of paddles for torrefaction of biomass at a commercial scale and have successfully shown its suitability to produce bio-coal briquettes [29], and Zinchik et al. studied the paddle reactors at lab scale and produced pyrolysis oils [30] and recently Kolapkar et al. [31] have studied a torrefaction-extrusion reactor and presented the thermo-mechanical properties of the torrefied pellets. In addition, extrusion has also been studied and has been used extensively in the plastic industry for several decades [32]. The integrated paddle and extrusion reactor used in this study, also referred to as torrefactionextrusion reactor, uses a single shaft, which mixes the waste blend, heats it, degrades the blend while removing chlorine, and finally extrudes it into uniform pellets. These pellets are ready to be used for combustion for power applications or upgraded to liquid/gaseous products and chemicals. This is a pilot-scale unit operating at a throughput of 800 t/yr. It has been developed by the team with the notion of scaling it up to a full commercial scale. The reactor-extruder part has been described in detail in the previous studies [26,31]. The current study provides comprehensive details on the integrated system and for each component, beginning from the waste processing stage all the way to the pellet storage, providing operation and energy data.

For the successful market implementation of torrefaction technologies, International Energy Agency provided the following key recommendations [20]: the need for production scale-up, end-user confidence, lower product price, standards for sustainability and traceability, product standards, and torrefying wastes. To substantiate that this technology addresses these recommendations for future market implementation, we performed Techno-Economic Analysis (TEA) and Life-Cycle Assessment (LCA). The TEA for the torrefaction-extrusion system is aimed at deriving the product cost at a commercial scale. Literature was surveyed for understanding the comparative cost of delivered torrefied biomass and mixed fiber-plastic wastes.

Costs of biomass torrefaction have been extensively studied [33,34] (and references cited therein), showing that the cost of biomass is a significant contribution to the overall cost. Whalley et al. [35] indicated that in the U.S., the delivered cost of biomass ranged from \$8–\$82/green tonne, International Renewable Energy Agency states that the cost of forest residues and wood waste range between \$10 to \$30/t while energy crops (corn stover, straw) cost \$39–\$60/t. Wright et al. [36] estimate the cost of biomass (corn stover) to be \$83/t. It is observed that biomass cost largely depends on the type of biomass, production source, and transport cost and has been reported as high as \$110/t [34] based on these factors. If this feedstock cost is further normalized based on moisture content and the mass loss in the torrefaction process, the cost of

biomass per tonne of torrefied material may increase further by \$60-80/\$ t torrefied material.

In contrast to biomass, a tipping fee is paid for wastes (MSW and industrial waste consisting of fibers and plastic). U.S. average tipping fee ranges from \$50.87–\$55.72 per U.S. short ton (1 U.S. short ton = 0.907 metric tonne) [37]. Assuming that the torrefied fiber-plastic waste product requires 1.5 times the incoming waste [10,25], considering the moisture content and mass loss required, the average tipping fee per tonne of torrefied product increases to \$84.11–\$92.13. In terms of economics, for feedstock cost/t of torrefied fuel, the use of fiber-plastic wastes can be a considerable incentive compared to biomass (negative  $\sim$ \$83/tonne vs.  $\sim$ \$60/t, a difference of  $\sim$ \$143/t). This number may increase even further if the cost per energy basis is factored in, as plastic in the wastes adds to the blend's overall heating value. Thus, using fiber-plastic wastes has not only significant economic benefits but also operational and safety benefits. The TEA provided in this study provides the cost of the product based on the capital and operating costs.

In addition to the technical and economic feasibility, the environmental sustainability of the process and product should also be considered. Untreated or improperly treated, fiber-plastic wastes can have detrimental environmental as well as health impacts [38]. With growing awareness about the environmental impacts of processes, LCA has become a popular tool to quantify the environmental impact. An LCA study by Sauve et al. estimated the environmental impact of landfills for MSW and showed  $\rm CO_2$  emissions ranged between 124 and 841 kg  $\rm CO_2$  equivalent/t [2]. Dong et al. studied the impact of incineration and pyrolysis and reported 416 kg  $\rm CO_2$  equivalent/t for the incineration process and 420 kg  $\rm CO_2$  equivalent/tonne emission for pyrolysis [39]. Recent work on MSW conversion to liquid transportation fuels indicates that MSW can serve as a feedstock to produce fuels and chemicals with favorable environmental profiles compared to conventional fossil products [40].

It should be noted that moisture is present in the fiber-plastic wastes. Our current system can handle moisture content of up to 10%. Any content above that value should be handled by an additional dryer, which is not included in this study. The inclusion of a dryer should affect both LCA and TEA.

Overall, the current study documents (a) the development of a proposed solution to address the issues described; (b) conduct TEA; and (c) conduct LCA of the mixed fiber-plastic waste torrefaction system. We explore the development and production of torrefied pellets from presorted plastic and fiber wastes, which can be utilized as a fuel to produce heat and power. This study includes (i) data from an integrated pilot-scale system operating at up to  $\sim\!800$  t/yr producing pellets, and (ii) TEA and LCA for a commercial scale 100,000 t/yr system, which includes a heat management system where the torrefaction gas stream (comprising some heating value) is burnt in a furnace, and the flue gases are used for drying and process heat [29].

### 2. Materials and methods

### 2.1. Materials

The blend of fiber-plastic wastes material was supplied by Convergen Energy (CE) LLC. It was shredded using various-stage shredding process from as-received material on the tipping floor, see Fig. 1(a), to  $\leq 50$  mm, see Fig. 1(b). Shredding is accomplished first by a Vecoplan RG-98 to  $\leq 300$  mm, then by Vecoplan VAZ-2500 to  $\leq 50$  mm. The feedstock is a blend of fiber-plastic wastes presorted by removing stones, glass, and metals. The shredded material was adjusted to provide consistent heat content of 25 MJ/kg, by tuning the fiber-to-plastic ratio, commonly requiring 60%–40%, fiber-to-plastic blend. After this shredding stage, the received material's density (as received from Convergen Energy and shown in Fig. 1a) is between 40 and 70 kg/m³. Further shredding was carried out to a size of  $\leq 3$  mm at the pilot plant using Allegheny 16-75CX, see Fig. 2(a). The material's density after this shredding stage is



Fig. 1. (a) Presorted mixed fiber-plastic 'as-received' on the tipping floor; (b) mixed fiber-plastic after three-stage shredding to size ≤50 mm.

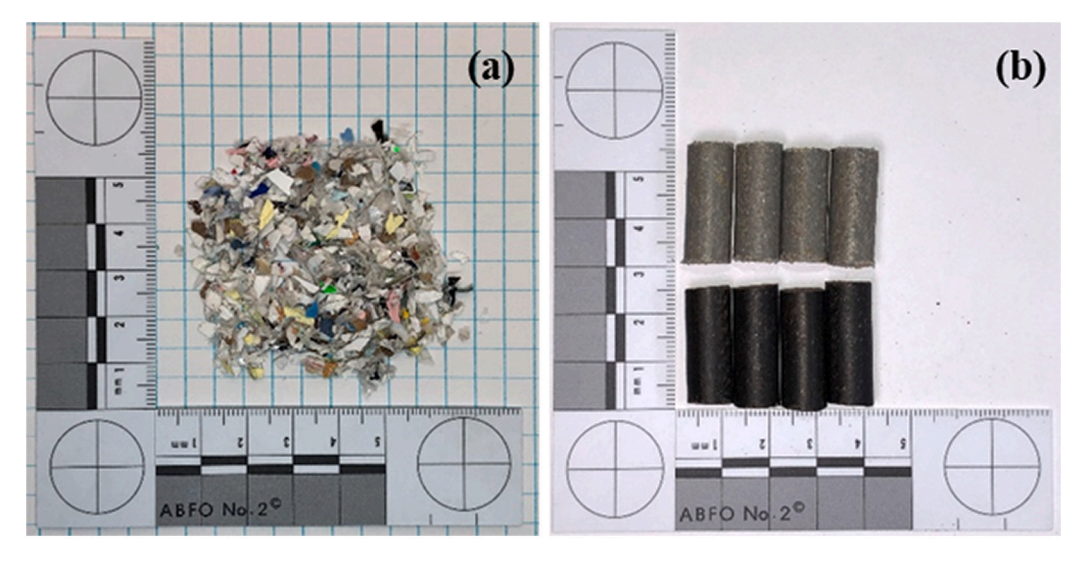
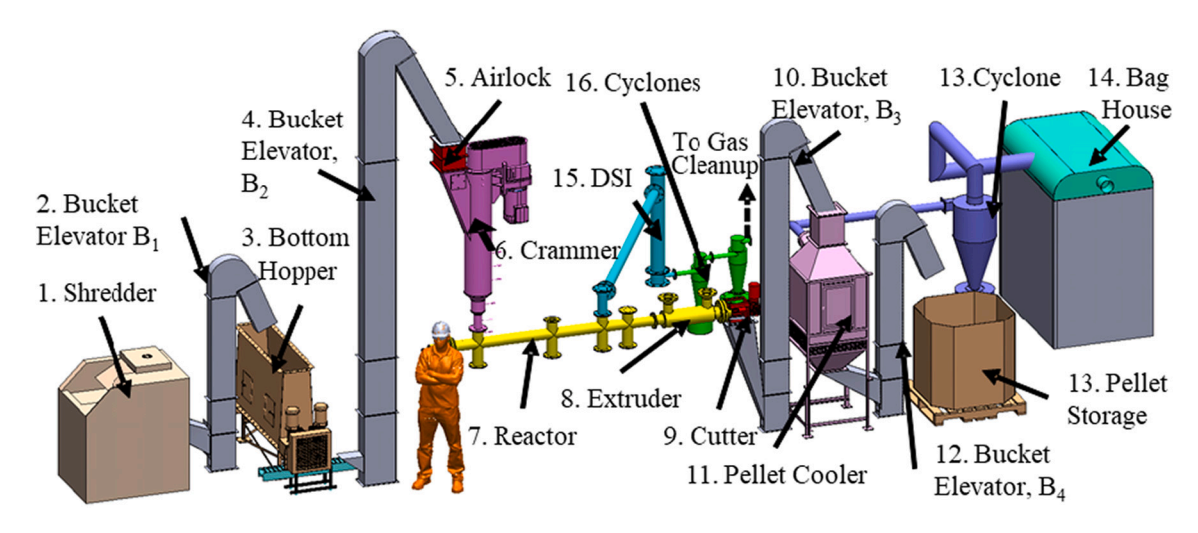


Fig. 2. (a) Mixed fiber-plastic waste after shredding to  $\leq 3$  mm, and (b) Pellets produced in the pilot-scale system using the mixed fiber-plastic waste at different levels of torrefaction.

between 105 and 120 kg/m $^3$ . Pellets produced using the integrated torrefaction-extrusion are shown in Fig. 2(b). The pellets presented show two different levels of torrefaction extent.

FTIR spectroscopy was used to identify the types of fiber and plastics present in the blend of incoming materials using a Thermo-Scientific

Nicolet Summit Pro spectrometer with an attenuated total reflection (ATR) accessory (Zn—Se crystal, iD5). Hundreds of randomly chosen pieces were analyzed using the OMNIC V-9 software package, plastic standards (low-density polyethylene from Rainer Plastics, Inc., high-density polyethylene from Equistar Petrothene LB01000, and



 $\textbf{Fig. 3.} \ \ \textbf{Scheme of the pilot-scale torrefaction-extrusion process.}$ 

polypropylene (PP) from Amcor), and Aldrich, Hummel, and Nicolet spectral libraries. The main types of the plastics identified using an FTIR analysis were Low-density Polyethylene (LDPE), High-density Polyethylene (HDPE), Polypropylene (PP), Polyethylene Terephthalate (PET), and traces of Polyamides (Nylon), while identified fibers mainly comprised of paper, cardboard, and carton. Detailed physical and thermo-mechanical characteristics of the biogenic (fibers, paper, etc.) as well as the plastic portion of the feedstock used in this work are detailed in our earlier study [10,25]. Additional insights on the chemical kinetics of fibers are presented in our separate past study on fiber wastes [9,27].

# 2.2. The pilot-scale integrated torrefaction-extrusion system

The scheme of the integrated torrefaction-extrusion system is presented in Fig. 3. The feedstock is introduced in a shredder (1) where it is downsized to a  $\sim$  3 mm size and then conveyed using bucket elevator  $B_1$ (2) to a live bottom hopper (3) that monitors the feed rate further downstream. This is followed by material conveying by a bucket elevator B<sub>2</sub> (4) into crammer (5) that preheats and densifies the material and creates an air seal preventing air from entering the reactor (6). The material then flows into a paddle reactor (7), where it mixes well, heats up, and undergoes a thermal decomposition through torrefaction. The torrefied material in the reactor flows into the extruder (8), densifying it into long rods. The extruder temperature is controlled by a heating/ cooling system (not shown) using oil (Therminol XP) as heat transfer fluid. The long rods are cut into pellets of predetermined size using the cutter (9). Note that the reactor is continuously purged by nitrogen (not shown) to ensure an oxygen-free environment, and an induced-draft (ID) fan removes the off-gases into a furnace that burns the organic material in this stream. The cut pellets are conveyed using a bucket elevator B<sub>3</sub> (10) to the pellet cooler (11) for cooling. The cooled pellets are conveyed again using bucket elevator B<sub>4</sub> (12) to the pellet storage box (13). We note that the extruder outlet also acts as an airlock to prevent air from entering the reactor. The gas stream generated from the torrefaction process is cleaned by passing it through Dry Sorbent Injection (DSI) (15) and two cyclones (16) connected in series to a gas cleanup system (not shown). We note that the gas stream can be utilized to provide some of the process energy. The following sections detail each of the key components of the system.

# 2.2.1. Shredding

Downsizing was found to be an essential pre-process for torrefaction and extrusion. Low-shear shredding allows the material to be downsized to  $\sim\!3$  mm flakes without 'fluffing up' - a volumetric expansion effect caused by the presence of fibers. The main advantages of the low-shear downsizing approach are: (i) up to three times density increase, thus reducing downstream components' size; (ii) prevents the formation of very-low-density fluffy material caused by high-shear shredding; (iii) produces a significantly more uniform blend than the incoming material, and (iv) reduces the material bridging tendency. Shredding to  $\leq\!3$  mm was accomplished by Allegheny cross-cut shredder model 16-75CX, using a 7.5 kW motor; a conveyor was used to feed the shredder, operating at a speed of 23 m/min. After passing through cutters, the material is cross-cut and reduced to a size of 3 mm broad stripes. Further reduction in particle size can be achieved using recirculation of material.

# 2.2.2. Live bottom hopper

Accurate material feeding is essential for the well-controlled torrefaction process. Fig. 4a shows the live bottom hopper developed and manufactured in-house for this purpose. The live bottom hopper has the following characteristics: (a) negative hopper angle, i.e., the width at the bottom is larger than the top with a 3° incline, (b) independently controlled variable pitch screws. The negative hopper angle avoids any occurrence of bridging during the material flow. The variable pitch allows maintaining a constant material level in the hopper. The weight of the bottom hopper is monitored continuously using four load cells (not

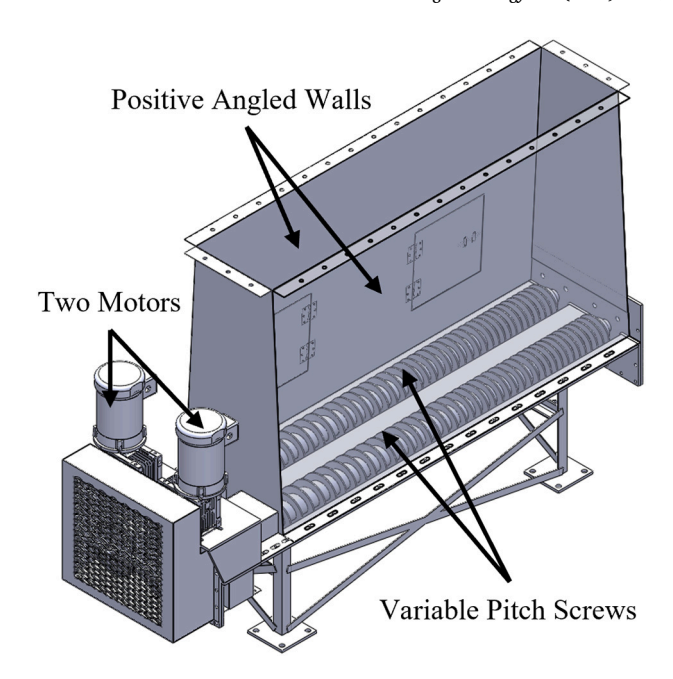


Fig. 4. Live bottom hopper with positive angles and independently controlled variable pitch screws.

shown) placed under the legs. Each leg has vibration insulating pads to insulate the motor vibration from the load reading.

#### 2.2.3. Bucket elevators

Four bucket elevators are used for conveying the material from one piece of equipment to the other. Bucket elevators are known for their suitability and reliability in conveying bulk material. The bucket elevators used in the system are U-series bucket elevators of various heights and capacities manufactured by Universal Industries, Inc.

# 2.2.4. Airlock and crammer

Continuous and stable feeding is critical for the operation of any fuelproducing facility. Wastes are known to have flowability problems such as bridging in hoppers due to various reasons like heterogeneity, different particle size, density, high moisture content, and compressibility [41]. A standard solution to this problem is to limit the type of material used or to use pneumatic or mechanical agitation techniques. However, neither provides an efficient solution for the mixed fiberplastic waste used in this study. We developed a crammer that can provide a constant mechanical agitation and direct the material downwards to deal with this issue and densify the material as well. Fig. 5 presents a schematic of the airlock and a crammer unit. The material is continuously fed by gravity from the top to the airlock. The airlock used in the system is an S8 series double-flap type airlock by Plattco $\ensuremath{\mathbb{R}}$  Corporation. One flap out of the two in the airlock is always in the closed position, allowing the airlock to maintain a positive seal constantly. The airlock is followed by material dropping in a sharp 70° angle crammer chute with polytetrafluoroethylene (PTFE) coating to prevent material buildup. The material is then received by a double helix auger that ensures proper and fast material feeding into the main chamber. As the material continues to flow, it is compacted with two-stage cross-section reductions from 0.30 m to 0.15 m and 0.15 m to 0.10 m, respectively. This reduction generates a higher friction coefficient that compresses the material from  $\sim 50 \text{ kg/m}^3$  to  $650-700 \text{ kg/m}^3$ .

The crammer is equipped with six external electrical heating elements, maintained at  $180-220~^\circ\text{C}$ , to dry (up to 10% moisture content) the incoming fiber-plastic waste and to help soften the plastics in the mix and form paste-like material, reducing friction with the crammer's walls. The crammer temperature was selected according to a differential

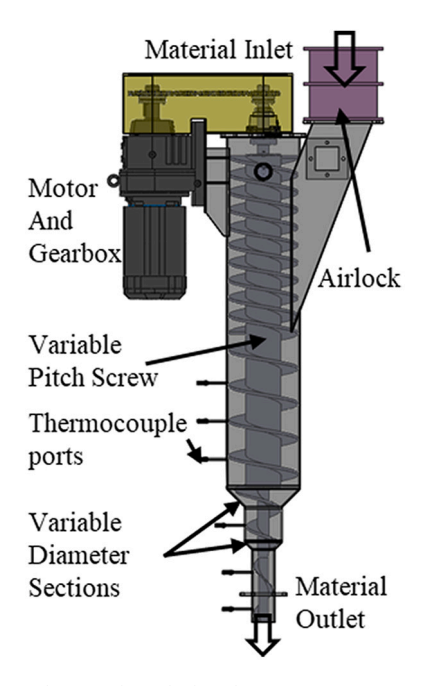


Fig. 5. Schematic showing the airlock and various components of the crammer.

scanning calorimetry (DSC) measurement that indicates phase transition (melting) of the major plastic components. One of the major advantages of crammer is its 100% fill rate which leads to a compact footprint, high rate of heat transfer, the ability to dry the material to yield a uniform paste and input material into the mouth of the reactor at a high mass feed rate. It is important to note that the crammer requires plastic for operation; it does not work with 100% fiber; experiments show that at least 10–15% plastic is required to enable smooth working.

# 2.2.5. Torrefaction-extrusion reactor

The fiber-plastic waste material is mixed, heated, torrefied, and extruded to produce rods before being cut into pellets. Fig. 6 shows the integrated torrefaction-extrusion reactor. It is described in detail in a previous study [31]; a brief description is provided below for convenience. The reactor is made of a 4-in. diameter shell externally heated by a series of electrical heaters. The shaft, 1.5 in. in diameter, is made from 15-5PH stainless steel. The reactor is designed with 4 zones: (i) transition zone; (ii) heating-reaction-grinding zone; (iii) feed zone (preextrusion); and (iv) extrusion zone. Each zone is designed to address a unique problem. Zone (i) addresses the feeding-related issue, ensuring a smooth and fast transition from the inlet of the reactor to the next zone. Zone (ii) is designed to maximize residence time and increase the mixing of the materials. As residence time and temperature determine the rate and extent of torrefaction, this design has significantly improved residence time by up to a factor of 3 compared to a regular screw reactor [31]. Enhanced mixing has been proven to improve heat transfer from the walls and radial temperature uniformity [26]. Zones (iii) and (iv) compact the material to a density suitable for storage and transportation while maintaining a low L/D ratio. At the end of the extruder, the material is guided to the die using a unique die design. The compressed material at the die also creates a plug, or an airlock, preventing oxygen penetration into the reaction area. While torrefaction occurs at  $250-350\,^{\circ}\text{C}$ , extrusion temperature is critical for ensuring optimal pellet quality, occurring at  $160-180\,^{\circ}\text{C}$ , which requires efficient cooling (described following).

We note that in a regular torrefaction plant, each of the abovementioned functions is carried in a separate reactor or component [42]. The plastic in the blend is enabled to carry all these stages (heating-reaction-grinding and extrusion) in one reactor by one shaft as the plastic turns the blend into a paste after melting.

The extruder temperature was controlled by an oil heating/cooling system using mineral oil due to its high heat capacity and safety characteristics. The system used for temperature control was manufactured by Heat Exchange and Transfer Inc., PA, USA, using Therminol XP® oil. During the startup, the oil is heated using an inbuilt 15 kW heater, while during the operation, it is cooled using a 73 kW capacity oil to the water heat exchanger.

#### 2.2.6. Cutter

Pellet cutting is essential in the pelletization process. The ring die produces multiple rods (8-hole, 0.5-in. diameter) that must be cut to produce pellets. Fig. 7 shows the cutter, with multiple blades developed for throughput up to 200 kg/h. The cutter is attached to the extruder with its spring-tensioned blades to maintain contact with the outer surface of the ring die. The blades are manufactured from tool steel alloy and are thermally treated to a hardness of HRC 55 for extended life and reduced blade dullness. To produce a uniform length of pellets, the rotation speed of the cutter is coupled using a PLC code with the die pressure measurement, as for a given material and temperature, extrusion velocity is a function of die pressure.



Fig. 7. Scheme showing the cutter.

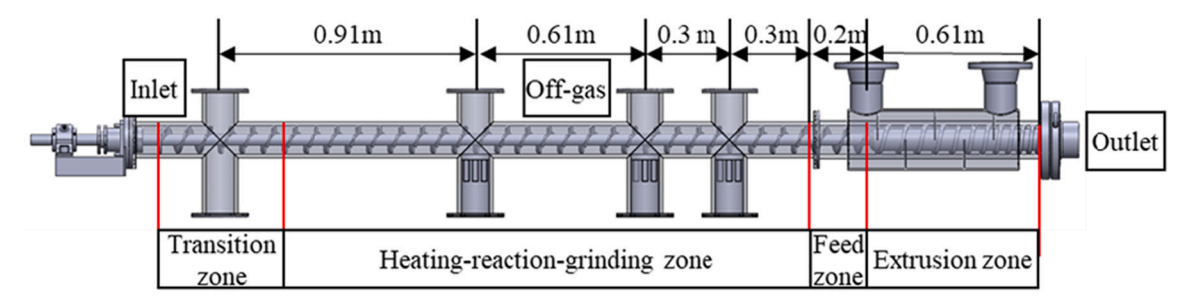


Fig. 6. Integrated torrefaction-extrusion reactor showing the scale and various zones.

# 2.2.7. Pellet cooler

Pellets exit at a temperature in the range of 160–180  $^{\circ}\text{C}$  and must be cooled before storage and transportation. A commercial counterflow cooler of 500 kg/h capacity manufactured by Münch-Edelstahl GmbH is used as part of the system. Pellets are conveyed from the cutter by a bucket elevator into an airlock on the top of the cooler. This is followed by a gravity drop of pellets into the cooler, where air enters from the sides, counter flows and is dragged by a blower through a cyclone (to collect fines). Air then passes through a bag filter to block particulates under 0.5  $\mu m$  from being released into the environment.

# 2.3. Mass flow rate and energy measurements

To measure mass flow rate and energy required to operate each component in the system, the following five parameters were measured: (i) moisture content before and after the process, (ii) weight measurement of feedstock (inlet), and the pellets produced (outlet) (iii) heat content of the pellets (iv) process heat used by the crammer and reactor units (v) specific electrical energy for the live bottom hopper, crammer, reactor, cutter, bucket elevator, and the pellet cooler.

**Moisture**: was measured using HFT 1000 Moisture Analyzer by Data Support Inc. Minimum of five measurements were performed per batch to have accurate moisture measurement. This facilitates the measurement of the mass lost in the form of vaporization of water during the torrefaction. The moisture content was measured for the feedstock  $(m_{moisture\ in})$  and for the produced pellets  $(m_{moisture\ out})$ .

**Mass flow rate**: was determined by measuring the weight using load cells manufactured by Omega (Model: TWA5 series), placed under: (i) bottom hopper and (ii) pellet cooler. This allows the measure the net feed  $(\hat{m}_{netfeed\ in})$  entering the reactor using Eq. (1).

$$\dot{m}_{netfeed\ in} = \dot{m}_{feed:in} (1 - \%moisture\_in) \tag{1}$$

where  $\dot{m}_{feed\_in}$  is the feedstock entering the crammer including the moisture and %moisture\_in is the measured % of moisture in the feedstock. The final weight of produced pellets is measure using Eq. (2) below

$$\dot{m}_{netfeed\_out} = \dot{m}_{feed\_out} (1 - \%moisture\_out)$$
 (2)

where,  $\dot{m}_{feed\_out}$  is the feedstock in the storage unit after cooling and % moisture\_out is the measured % of moisture in the pellets.

The mass lost to the gas stream in the torrefaction was calculated using Eq. (3),

$$Mass \ Loss = 1 - \frac{\dot{m}_{netfeed\_out}}{\dot{m}_{netfeed\_in}}$$
 (3)

Heat content: was measured before and after torrefaction using a bomb calorimeter (Parr Instrument Company, Model 6100). A typical experiment involved a 1 g grounded mixed waste sample placed into a porcelain crucible. The bomb was then filled with oxygen (~400 psi) and was submerged into a jacket filled with 2000 g of distilled water. The sample was ignited, and the heat released was measured in the form of the temperature difference of the water in the jacket before and after the combustion. The relation between the heat and chlorine (a crucial pollutant of interest for solid fuel users) content with respect to mass loss was studied [9,10,25] and is summarized in the Results section. The mass loss and chlorine content of the same material torrefied in a batch reactor and the continuous pilot-scale reactor are compared. Instead of temperature and time, mass loss is used as a universal variable [9,10,25] to present the heat and chlorine content results for torrefaction.

**Process heat:** As electric heaters are used to heat the crammer and the reactor, the process heat utilized was measured by multiplying the percent duty cycle (defined as the time the heater is on over the cycle time) of the electric heaters and the maximum power of the heaters. This allowed the measurement of the process heat utilized by the crammer and the reactor at specific feed rates and temperatures. More details

regarding the configuration of heaters are presented in the previous study [26,31].

Specific electrical energy (e): can be defined using Eq. (4),

Specific Electrical Energy (e) = 
$$\frac{Energy\ consumed}{Mass\ flow\ rate\ (m)}$$
 (4)

where e is the specific electrical energy required to drive each of the motors in the system (for the shredder, live bottom hopper, bucket elevators, crammer unit, reactor unit, and the cutter) and  $\dot{m}$  is the mass flow rate through the equipment.

The live bottom hopper, the reactor, and the crammer are controlled using a variable frequency drive (VFD), which provides the required electrical information, and  $\dot{E}$  was measured as a function of mass flow rate. The bucket elevators and the pellet cooler were not operated by VFDs, and a current transmitter was connected to their power supply for measuring their e. All the data was processed using a commercially available Series-P3 PLC (by Automation Direct) unit. The Indusoft V8.1 HMI software was used as the data acquisition system.

For the shredder,  $\it e$  was measured using three different materials: (a) plastic films ( $\rho=35.16~kg/m^3$ ), (b) mix fiber-plastic films ( $\rho=76.17~kg/m^3$ ), and (c) mix fiber-plastic fines ( $\rho=263.34~kg/m^3$ ) to understand the effect of density and different shredded materials. The current was measured at every 0.25 s. The mass flow rate was increased from 0 kg/h to flood feed (max) for each material in increments of 30 kg/h.

For the live bottom hopper, e was measured using mix fiber-plastic films ( $\rho=76.17~{\rm kg/m^3}$ ). The bottom hopper has been tested with several different materials during past experiments; the aim here is to demonstrate the consistent flow of material using the rotation frequency (rpm) vs. mass flow rate plot. To measure the specific energy consumption current was measured at a frequency of 4 Hz. The mass flow rate was increased by increasing the frequency by 15 Hz intervals. All the experiments were triplicated.

For the reactor, e was measured for fiber-plastic wastes in the earlier study [31]. It has been summarized in the result section. The details about measurements for crammer and other equipment are specified in the Results section.

# 2.4. TEA process modeling for commercial scale

The unit discussed in this study was designed and developed with commercialization in mind. To assess the economic viability of this technology, this study shows the TEA of the commercial system. The objective of the TEA is to assess the cost of a complete commercial-scale torrefaction plant, of 100,000 t/yr, based on this pilot-scale technology.

# 2.4.1. Process modeling boundary

The system boundary for the TEA encompassed processes and equipment delineated in Fig. 8.

A loader delivers waste materials to an infeed belt, following which the materials undergo size reduction using a three-stage shredding process. Using a live bottom hopper and bucket elevator, the materials are then conveyed to a system that distributes the material into four identical reactor-extruder-cutter setups that perform the torrefaction process and cut the extruded rods. Material coming through the four streams is combined using a pellet collection. A bucket elevator then conveys the material into a cooling process, following which the preprocessed materials are conveyed into storage. The system boundary for the TEA does not include building or land costs because they depend strongly on location.

# 2.4.2. Cost estimation methodology

The Idaho National Laboratory's (INL) Biomass Logistics Model (BLM) was used to estimate biomass feedstock logistics cost and energy consumption estimates. The BLM utilizes an approach that combines methodologies described by the American Society of Agricultural and

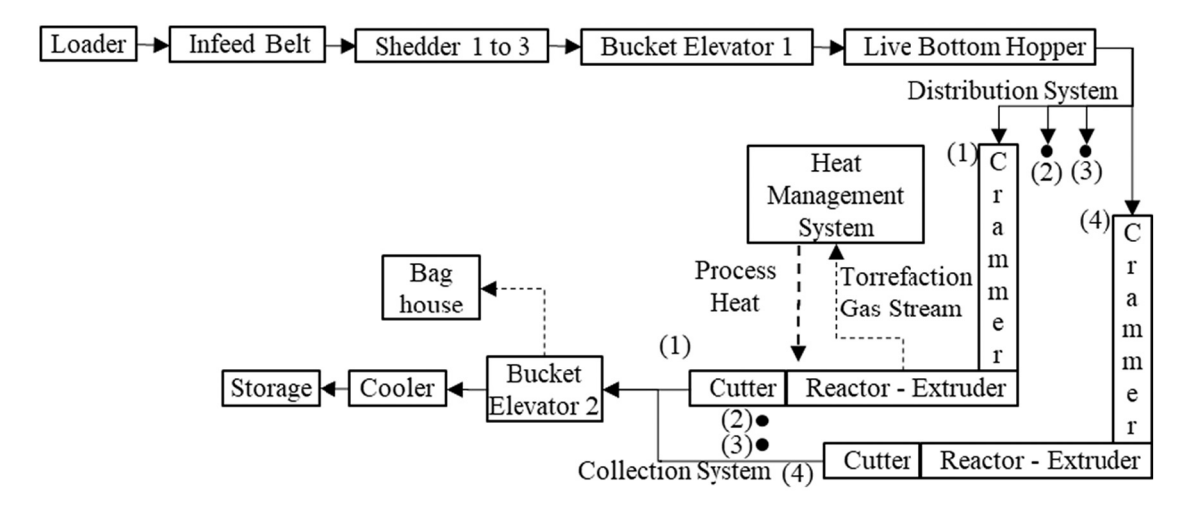


Fig. 8. Simplified block diagram of the commercial scale torrefaction process.

Biological Engineers [43] and Agriculture and Applied Economics [44]. These methodologies encompass cost estimation procedures for agricultural machinery management ranging from equipment performance, field efficiency, repairs and maintenance, fuel and lubrication, insurance, housing and taxes, labor, as well as capital recovery calculations to compute the annualized value of capital [43,44]. The BLM analytic engine is built in the systems dynamic's software package Powersim<sup>TM</sup>. The BLM is designed to work with various biofuel conversion platforms and accommodates a range of feedstock types.

In this study, we incorporated information from a collection of databases that provide a) engineering performance data for hundreds of equipment systems, b) spatially explicit labor cost datasets, and c) local tax and regulation data. We simulated the flow of feedstock through the entire supply chain while tracking changes in feedstock characteristics (i.e., moisture content, dry matter, ash content, and dry bulk density) and calculating cost and energy consumption [45]. Plant level costs, including installation, personnel (operators, engineers, and maintenance staff), and maintenance costs, are added to the per tonne cost of pre-processing estimated using equipment-related data, financial assumptions, and energy usage data.

# 2.4.3. Assumption and cost breakdown

It is assumed that this unit can produce 100,000 dry tonnes of torrefied materials annually, at 24 h/day and 350 days/yr. Operational parameters used in the TEA are listed Table 1, whereas general and equipment-related assumptions based on teams' procurement and construction experience of similar-sized equipment are listed in Table 2.

# 2.5. LCA process modeling for commercial scale

The goal and scope of the LCA portion of this study are to determine the environmental impacts of the torrefied product, produced in a full commercial-scale torrefaction plant, of 100,000 t/yr, based on this technology. The environmental impacts can be compared to other studies of similar materials to compare the specific torrefaction processing or to other intermediate products to illustrate the environmental

**Table 1**Operation parameters used for the TEA.

Operation parameters	Value	Unit
Annual production	100,000	dry tonnes/yr
Required raw materials	151,976	wet tonnes/yr
Annual operation days	350	days/yr
Daily operating hours	24	hrs/day
Initial moisture content (W.B.)	6%	
Final moisture content (W.B.)	0.1%	

**Table 2**General assumptions made for the TEA. Costs are presented in 2020\$.

Interest Rate = 8%
Insurance and Tax = 2%
Maintenance = 3% of Capital and Installation costs
Electricity cost = 0.065 \$/kWh
Natural gas cost = 7.55 \$/MMBtu

Diesel cost = $2.55 $ \$/gal		
Equipment	Machine life	Purchase price
Loader	6 years	\$250,000
Infeed Belt	15 years	\$50,000
Three-stage Shredder	5 years	\$6,000,000
Live Bottom Hopper	15 years	\$250,000
Bucket Elevator	15 years	\$100,000
Distributor	15 years	\$100,000
Crammer and Torrefier	15 years	\$350,000
Cutter	10 years	\$50,000
Pellet Collector	15 years	\$200,000
Cooler	15 years	\$100,000
Conveyor to Storage	15 years	\$100,000
Heat Management System	15 years	\$750,000
Gauges and Analyzers	15 years	\$750,000

tradeoffs associated with using this MSW-derived intermediate instead of fossil-based or bio-derived products. The environmental impacts of interest in this work are cumulative greenhouse gas (GHG) emissions, often described as the global warming potential of the process, and fossil energy demand. Wood chips from forest residues are used as a comparable product. The system boundary of the LCA study will include the loading and size reduction of the fiber-plastic waste before torrefaction, as described above, but does not include collection and transport because this collection and transport activity would still be occurring in the same fashion if the municipal solid waste was still being taken to a landfill. The LCA study will incorporate the impacts of diverting the fiber-plastic wastes from their prior fate, assumed to be disposed of in a landfill. Torrefaction operations and emissions are included in the system boundary. The waste contains a mixture of materials, some derived from biogenic carbon (such as paper, carton, cardboard), and some derived from fossil carbon (plastics). When accounting for GHG emissions of these bio-derived products, it is common to account for the carbon initially sequestered from the atmosphere when the bio-based products were created and then add in the emissions of carboncontaining gases released from the system along each subsequent process in the system boundary. We have done that carbon accounting here to facilitate a comparison with the forest-based wood chips, which are also bio-based and remove carbon from the atmosphere as they are made into an intermediate wood chip product. In the absence of this torrefaction system, the waste is assumed to be sent to a landfill, where a

portion of the biogenic carbon is converted to methane and carbon dioxide, while a portion of the biogenic carbon is effectively sequestered in the landfill along with the fossil-derived carbon. When the waste avoids the landfill and is sent instead to the torrefaction system, avoidance of the landfill carbon emissions and biogenic carbon sequestration is also included in the system boundary of this LCA. Landfill carbon dynamics change over the landfill's life and can vary considerably based on the landfill operating conditions and the surrounding climate. In the current study, landfill carbon assumptions were developed using the GREET 2019 spreadsheet LCA tool [46], using IPCC reference data and assuming an actively managed landfill with a landfill gas collection efficiency of 45%, and a subsequent flaring of the collected gas at 95%conversion to CO<sub>2</sub>. The primary uses for the torrefied pellet would likely be as a feedstock for future processing into fuels and chemicals. For this study, we establish a functional unit for the LCA as the MJ of energy present in 1 kg of torrefied product (31.4 MJ). For the forest-derived wood chip comparison product, which has an assumed lower heating value of 16.3 MJ/kg [47], 1.93 kg of wood chips would be needed to provide the same level of service as 1 kg of torrefied pellet.

**Table 3**Key life cycle input data and assumptions.

Item	Baseline scenario	Forest-derived wood chip comparison	Comments
Material composition	57% Paper (43.5% C), 38% Plastic (60% C), 5% Ash (0% C)	100% wood (50% C)	Represents 60/40 distribution between paper and plastic as described above in MSW description.
Lower Heating Value of product	31.4 MJ/kg	16.3 MJ/kg dry chips	Based on the initial composition of MSW, with 18% energy loss and 30% mass loss during torrefaction.
Fuel consumption	0.226 MJ/kg product	0.641 MJ/kg dry product	MSW: Based on fuel consumption of 4 loaders for 8400 h/yr at 4.7 gals/h; Wood chips: Based on collection, processing, and transport assumptions from [51]
Electricity consumption	0.23 MJ/kg product	0	Based on unit operations described in Table 7. The energy consumption by equipment type is presented in Table 7. It can observed that Shredding and Crammer-Torrefaction units are largest energy consumers.
Natural Gas consumption	0.0006 MJ/kg product	0	For periodic torrefaction startup, averaged over the full year of operation
Landfilling assumptions (prior fate)	19.3 g CH <sub>4</sub> /dry kg MSW, 231 g CO <sub>2</sub> /dry kg MSW, 139 g biogenic C sequestered/dry kg MSW	N/A	Disposal to the landfill with 45% landfill gas collection efficiency, flaring of LFG at 95% efficiency - these carbon flows are avoided as a result of MSW diversion to torrefaction system [46]

#### 2.5.1. Life cycle inventory development

Table 3 shows key life cycle inputs and key assumptions for the base case scenario and the forest-derived wood pellet comparison. LCA modeling was performed in the SimaPro modeling software, using the Ecoinvent version 3 database of inputs [48] to generate the entire life cycle inventory for each scenario. Electricity impacts were generated by modifying the standard US electricity eco profile for medium-voltage electricity present within Ecoinvent by updating it to include the most current distribution of the electricity grid mix from the U.S. EPA E-grid database [49], which consists of 23.3% coal, 38.4% natural gas, 19.6% nuclear, 6.8% hydroelectric, 7.1% wind, and other minor components as the most current U.S. reference case. This modification resulted in an electricity mix that had a  $\sim 40\%$  lower GHG emissions profile than the standard Ecoinvent version 3 data with reference data from just seven years earlier (2019 vs. 2012), which is an impressive change in a relatively short period. Carbon losses during torrefaction processing were estimated to be 8% of dry MSW weight, based on prior modeling work in this area [50].

#### 2.5.2. Life cycle impact assessment

Life cycle impacts were assessed within SimaPro using the IPCC 100a method to assess the global warming potential of the scenarios, expressed as kg of  $CO_2$ -equivalent emissions from all climate-active gases including  $CO_2$ ,  $CH_4$ , refrigerants, and others. The cumulative energy demand method was used to determine the nonrenewable fossil energy demand of the scenarios in MJ fossil energy per kg of product.

#### 3. Results and discussion

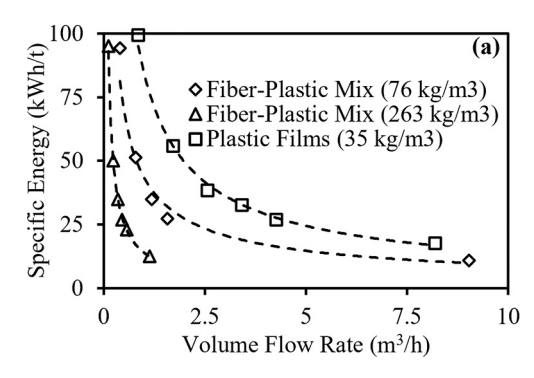
#### 3.1. Pilot scale system

# 3.1.1. Shredding

The energy required to operate the shredder, which operates at low shear, was measured for various materials at various densities. Three different materials: plastic films ( $\rho = 35.16 \text{ kg/m}^3$ ), mix fiber-plastic material ( $\rho = 76.17 \text{ kg/m}^3$ ), and mix fiber-plastic ( $\rho = 263.34 \text{ kg/m}^3$ ) were tested. Most plastic and fiber wastes in all the different materials are films with thickness typically ranging between 0.05 and 2 mm. The specific electrical energy consumed as a function of mass flow rate allows us to calculate the shredding cost for the shredder's operation. Fig. 9(a) shows the specific energy consumed by the shredder vs. the volume flow rate, with the clear observation that the lower the density, the higher the electric specific energy consumption. It also implies that the lower the density, the larger shredder required for a given mass feed rate. Fig. 9(b) shows the specific energy consumed by the shredder vs. the mass flow rate, with the clear observation that it is not dependent on density; the specific energy consumption was similar across all the materials: it reduced from 100 kWh/t to 10 kWh/t.

### 3.1.2. Live bottom hopper

For the live bottom hopper, the key aim is to provide consistent dosing of the material. The rheological nature of the feedstock has a strong influence on the consistent operation of the live bottom hopper and its efficiency for accurate dosing. Klinger et al. and Idaho National Lab [41,52–54] thoroughly studied flow models, both computationally and experimentally, for biomass-based materials supported by measurements particle density, surface friction, elastic modulus, morphology (size and shape), internal friction, hopper wall friction angles, and hopper width. Assessing all these materials and the rheological properties of our wastes is difficult; however, we realized through numerous experimentations that the type of shredder and shape of the shredded material has the strongest influence on the flowability of the material. As indicated above, low shear shredders appear to generate flakes that flow better than high shear shredders. Further, stripe-shaped flakes were found to cause bridging, whereas square-shaped flakes prevent bridging. The angle of the walls of the feeder is also critical. Our



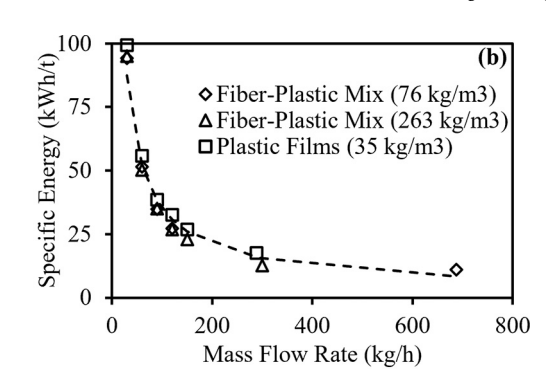


Fig. 9. (a) Specific energy vs. volume flow rate for the stage III shredder; (b) Specific energy vs. mass flow rate for the stage III shredder.

feeder was designed and constructed following these experiments and findings. The mass flow rate of a specific material vs. the rotation frequency was found to be an excellent indicator of the suitability of the feeder and the bridging propensity. Screw augers operating at flood-fed conditions are outstanding feeders providing a very accurate mass flow rate, provided no bridging occurs.

Fig. 10(a) shows the mass flow rate of striped shaped flakes (3 mm wide and 12 mm long) produced from our shredder when the material was shredded in a single pass. Clearly, the mass flow rate is irregular and cannot be used for conveying and dosing. When the striped material was passed a second time through the shredder, square flakes (3 mm by 3 mm as shown in the inset) were produced; the mass flow rate of this material is depicted in Fig. 10(b), showing a linear increase with the rotation frequency, with clear consistent material flow.

Fig. 11 shows the specific energy consumption of the live bottom hopper decreasing with the increase in the mass flow rate. For mixed fiber-plastic material with a density of  $149 \text{ kg/m}^3$  that was shredded to the size of 3-mm by 3-mm, Eq. (5) can calculate the specific energy:

$$e = 41.11 \times \dot{m}^{-0.34} \tag{5}$$

where, e is the specific energy consumed by the live bottom hopper, and  $\dot{m}$  is the mass flow rate of material from the live bottom hopper. The behavior of the specific energy for the live bottom hopper decreases with mass flow rate; for example, for a 1 t/h mass flow rate, the specific energy is 3.9 kWh/t.

# 3.1.3. Crammer

For the crammer, estimated electrical consumption (based on experimental runs) for a material compression factor of  $\sim\!17$  is at 40 kWh/t, and the heating requirement is 50 kWh/t. However, it is essential to note that the crammer load, and as a result, the specific electrical energy consumption is very sensitive to the rotation frequency of the crammer and the temperature setpoint. e vs. rotation frequency and e vs.

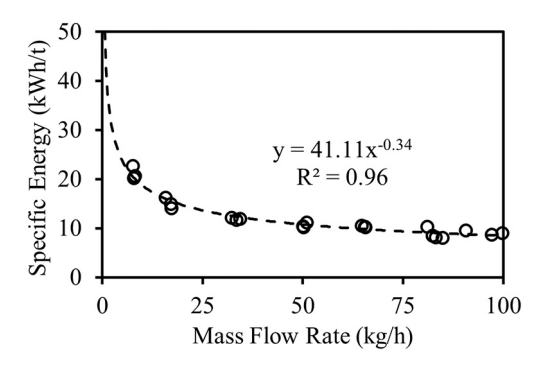
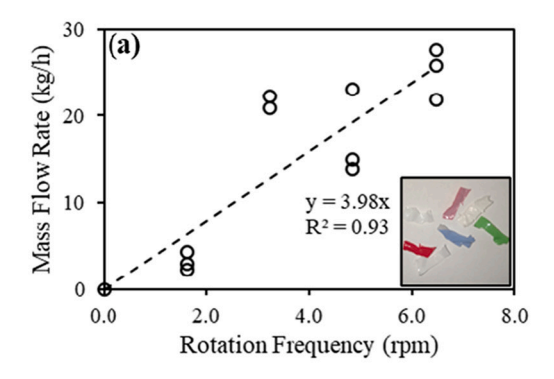


Fig. 11. Specific electrical energy (e) vs. mass flow  $(\dot{m})$  rate for live bottom hopper.

temperature has a strong non-linear correlation. During the experimentation, a sudden drop of load and energy consumption of  $\sim\!50\%$  is observed after the crammer frequency exceeds 10 rpm for 60:40 fiber plastic blend materials at 200 °C. This can be attributed to the factors like change in viscosity and several rheological factors. Thus, we believe the complex nature of the crammer behavior deserves a separate study to quantify the energy consumption relationship. However, to understand that average energy consumption at normal operating conditions is at the average value of 40 kWh/t reported above can be used.

The crammer temperature was selected from the DSC trace measured for the material used and shown in Fig. 12. The peaks represent an endothermic process attributed to phase transitions. The first peaks at around  $100-125~^{\circ}\text{C}$  are attributed to polyethylene (PE) melting; the peak around  $170~^{\circ}\text{C}$  is attributed to melting of polypropylene (PP); these two plastics constitute the majority of the plastic waste. The peal around  $250~^{\circ}\text{C}$  is attributed to polyethylene terephthalate (PET) melting. We selected to operate the crammer at  $180-190~^{\circ}\text{C}$  as both PE and PP



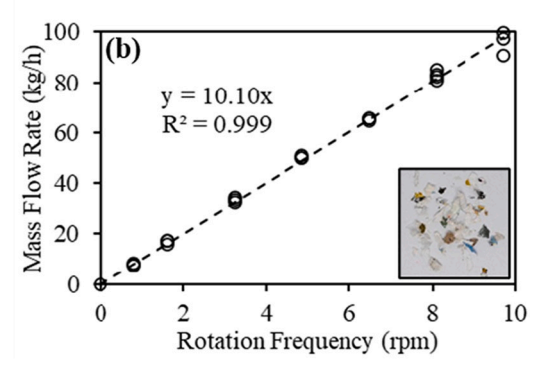


Fig. 10. Mass flow rate vs. rotation speed of live bottom hopper shaft for: (a) bridging material; and (b) non-bridging material. The inset in (a) shows the strip-shaped flakes material with a tendency to bridge, and the inset in (b) shows the square-shaped flakes.

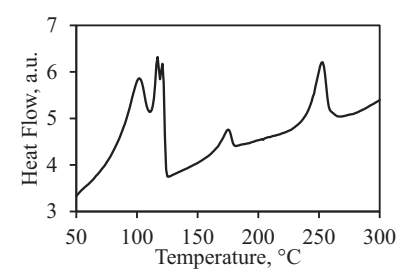


Fig. 12. DSC of fiber-plastic waste blend.

melted, and PET can be dissolved into them, thus creating a flowing paste.

# 3.1.4. Torrefaction-extrusion reactor

For the reactor, the specific mechanical energy of 335 kWh/t is required to convey and extrude the material at an average mass flow rate of 9 kg/h; it drops to 94 kWh/t at 50 kg/h, further drops to 12 kWh/t at 1 t/h. The correlation between the specific energy required and mass flow rate is presented in Eq. (6).

$$e = 1370 \times \dot{m}^{-0.684} \tag{6}$$

An additional 125 kWh/t of thermal energy is required to heat the material to 350  $^{\circ}\text{C}.$ 

#### 3.1.5. Bucket elevators

For the bucket elevators, the energy consumption was measured at 0.36  $\pm$  0.04 kWh/t for the pellets with a bulk density of 500 kg/m<sup>3</sup>

### 3.1.6. Cutter

For the cutter, the average energy consumption is 0.07 kWh with maximum consumption at 0.85 kWh. The power consumption is a function of the rotation frequency, which translates to pellet length and the type of material.

# 3.2. Mass balance

As described earlier, the mass balance is a tool to calculate mass lost in the torrefaction process. Fig. 13 shows the mass flow rate to the system measured by the load cells from the live bottom hopper and the output flow rate shown by the load cells under the pellet cooler. The figure shows that the slope of the plot of respective measurements represents the mass flow rate in and out of the system. The difference in their slopes denotes the mass lost during the torrefaction at the set conditions.

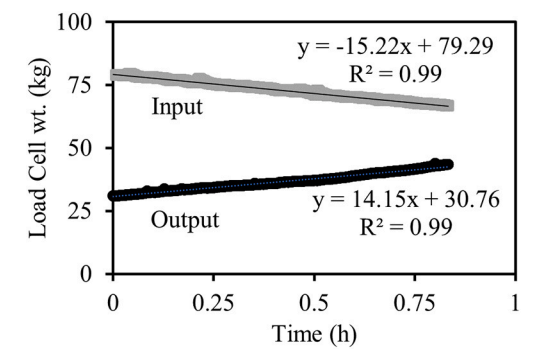


**Fig. 13.** Typical load cell measurements showing mass input at the live bottom hopper and mass output at the pellet cooler. Mass loss can be calculated from the difference in slopes (7% for the example above).

#### 3.3. Heat and chlorine contents

Fig. 14 shows the heat and chlorine contents of the 60% fiber and 40% plastic material from a lab-scale batch setup and pilot-scale continuous setup. It can be observed that instead of the specific temperature and residence time combination, mass loss can be used as a universal variable to quantify the heat and chlorine content of the material. It can be observed that with the increase in the mass loss from 0% to 50%, the heat content increases from  $\sim 25$  MJ/kg to  $\sim 34$  MJ/kg while the Cl content decreases by up to  $\sim 70\%$ . The ppm levels vary batch to batch; however, the Cl removal is independent of the initial ppm levels of Cl. Also, the Cl removal is a function of mass, and the type of reactor (batch vs. continuous) does not play a major role. Using this relationship expressed in Fig. 14, mass loss can be used as an indicator to derive the properties of the produced pellets and vice-versa. In other words, the mass balance is a simple method of mass loss measurement that can be used for online calculation of the properties of the produced pellets.

# 3.4. Commercial scale system TEA

Details of the above-described pilot-scale system can be used for the techno-economic and lifecycle assessments. Based on the assumptions and machine performance, the total cost of the system is estimated to be \$55.28/dry tonne (2020\$), which includes preprocessing costs at the equipment level and other plant-level costs comprising of installation, labor, and maintenance.

For the complete preprocessing and torrefaction stage, the cost breakdown is presented in Table 4. It indicates that the most important costs are attributable to the crammer and torrefier (\$10.08/dry tonne) and the three-stage shredder (\$8.38/dry tonne). The crammer and torrefier contributes 41.55% and the three-stage shredder contribute to 34.55% of the preprocessing and torrefaction stage cost.

At the plant level, annual labor costs (\$16.62/dry tonne) and installation costs (\$9.50/dry tonne) are the largest contributors to total costs presented in Table 5. Installation costs include costs incurred for installation, testing and commissioning, training of operators, costs incurred for engineering designs, and a 10% contingency reserve.

Energy requirements can be upscaled well using the various specific energy correlations found in the sections above. The capital costs are estimated from the pilot-scale costs and the experience the Michigan Tech teams acquired when building an 80,000 t/yr torrefaction facility [55]. Energy consumption by fuel types was estimated to enable LCA and is presented in Table 6. The system is designed to be self-sustaining, whereby the gas stream from the torrefaction process is utilized in the heat management system. However, approximately 48 MMBtu of natural gas is used in the start-up phase.

The energy consumption by equipment type is presented in Table 7. It can be observed that Shredding and Crammer-Torrefaction units are the largest energy consumers.

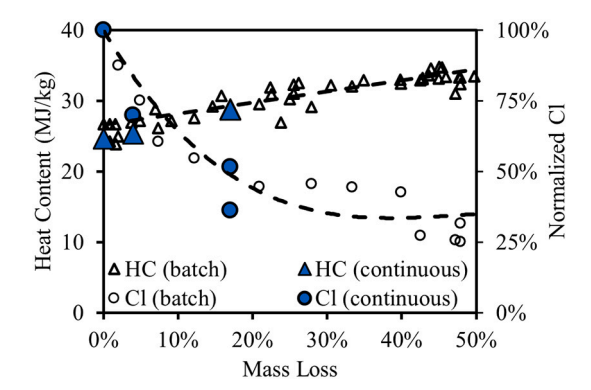


Fig. 14. Heat content vs. mass loss and normalized Cl content vs. mass loss using batch and continuous reactor setup.

**Table 4**Breakdown of costs for fiber-plastic pre-processing and torrefaction unit operations.

Equipment (All costs in 2020\$)	Cost (\$/dry tonne)	Cost (%)
Loader	\$1.56	6.45
Infeed Belt	\$ 0.08	0.32
Three Stage Shredder	\$8.38	34.55
Live Bottom Hopper	\$0.29	1.18
Bucket Elevator 1	\$ 0.13	0.55
Distributor	\$0.13	0.55
Crammer and Torrefier (4 units)	\$10.08	41.55
Cutter (4 units)	\$0.46	1.91
Pellet Collector	\$0.33	1.36
Bucket Elevator 2	\$0.17	0.72
Cooler	\$0.20	0.82
Conveyor to Storage	\$0.18	0.73
Heat Management System	\$ 1.14	4.72
Gauges and Analyzers	\$ 1.11	4.59
Total	\$ 24.25	100

**Table 5**Breakdown of total costs at the plant. Costs are reported in 2020\$.

	Cost (\$/dry tonne)
Capital cost per dry tonne	\$24.25
Installation cost per dry tonne	\$ 9.50
Labor cost per dry tonne	\$ 16.62
Maintenance cost per dry tonne	\$ 4.91
Total cost per dry tonne	\$55.28

**Table 6** Energy consumption by fuel type.

Fuel type	MMBtu/dry tonne
Diesel	0.0624
Electricity	0.2407
Natural gas	0.0006

**Table 7**Energy consumption by equipment type.

Equipment	Fuel/unit	Value
Loader	Diesel (gal/dry tonne)	0.45
Infeed Belt	Electricity (kWh/dry tonne)	0.38
Three Stage Shredder	Electricity (kWh/dry tonne)	33.06
Live Bottom Hopper	Electricity (kWh/dry tonne)	0.38
Bucket Elevator 1	Electricity (kWh/dry tonne)	0.38
Distributor	Electricity (kWh/dry tonne)	0.38
Crammer and Torrefier (4 units)	Electricity (kWh/dry tonne)	33.06
Cutter (4 units)	Electricity (kWh/dry tonne)	0.38
Pellet Collector	Electricity (kWh/dry tonne)	0.55
Bucket Elevator 2	Electricity (kWh/dry tonne)	0.38
Cooler	Electricity (kWh/dry tonne)	0.77
Conveyor to Storage	Electricity (kWh/dry tonne)	0.38
Heat Management System	Electricity (kWh/dry tonne)	0.38

<sup>&</sup>lt;sup>a</sup> The crammer-torrifier uses a small amount of natural gas during start-up.

# 3.5. Sensitivity analysis for TEA

The crammer-torrefier unit contributes nearly 42% of total preprocessing costs, we performed sensitivity analysis on three parameters price, energy usage, and throughput impacting this equipment to evaluate its influence at a system level.

Under the base case, the parameters are as follows: energy usage (33.07 kWh/t), the purchase price (\$350,000), throughput (4 crammer-torrefier units). We evaluated pre-processing costs wherein the parameters are  $\pm 25\%$  compared to the base case assumptions. Additionally, changes in the number of units of crammer-torrefier are accompanied by a change in the number of cutters as these two pieces of equipment are

used sequentially as per the system design. The results are presented in Table 8.

# 3.6. Commercial scale system LCA

Life cycle assessment results are shown below in Table 9 for GHG emissions and fossil energy demand of the torrefied pellet product and the wood chip comparison. Large CO<sub>2</sub> sequestration credits are observed for both products due to the large amount of biogenic carbon currently sequestered in the product. The credit is larger for each kg of torrefied pellet than for each kg of wood chip ( $-1.98 \text{ kg CO}_2\text{eq/kg pellet vs.} -1.83$ kg CO2eq/kg wood chip) despite the higher proportion of biogenic carbon in the wood chips, because in the torrefied product case we are also accounting for the avoided emissions that would have occurred if the MSW feedstock had been disposed of in a landfill, most notably the methane emissions that are a particularly potent greenhouse gas. Emissions of CO<sub>2</sub> during the torrefaction process are included and are a key component of the overall emissions profile, contributing roughly 20 times more to the global warming potential of the torrefied pellet than either the diesel fuel or electricity used in materials handling and preprocessing. The cumulative result is still negative for the torrefied product because the biogenic carbon credit and avoided landfill emissions are larger than process emissions at this intermediate stage of the overall use of this material. If the torrefied product were to be converted to a fuel product and combusted, those process and combustion emissions would have to be counted towards the full life cycle emissions of

Similarly, for the wood chip product, the emissions resulting from processing are important but still overcome by the significant biogenic carbon credit for wood sequestration of atmospheric carbon. Importantly, because 1.93 kg of wood chips are required for each kg of torrefied product to account for the equivalent functional unit (31.4 MJ of each product), this negative result in an intermediate stage assessment of the global warming becomes magnified in comparison to the torrefied product. When both products are converted to fuels and combusted, this apparent difference in the environmental profile may be reduced as the emissions are accounted for in all life cycle stages. The comparison is somewhat reversed when considering the fossil energy demand of both products. Fossil energy demand for the torrefied pellet (0.73 MJ/kg pellet) is due to the use of electricity (56%) and diesel fuel (44%) during the material handling prior to torrefaction. This impact is lower than the fossil energy demand associated with collecting and transporting wood chips (0.83 MJ/kg wood chips), and this difference is again magnified when the products are put on an equivalent basis with the same functional unit. Wood collection and transport are highly sensitive to the specifics of the operation, including the equipment mix used and the transport distance [56], so specific inputs related to a particular operation would make the comparison useful when assessing the relative merits of one feedstock over another. However, in general, it appears that the MSW-derived torrefied pellet can have a favorable profile when compared to biogenic feedstocks.

# 3.7. Sensitivity analysis for LCA

Table 10 presents the sensitivity analysis for the LCA. The environmental impacts of the MSW-derived pellet are expected to be sensitive to both the material composition of the MSW and the assumptions made

**Table 8**Sensitivity analysis for crammer-torrefier unit. Costs are reported in 2020\$.

	Total cost (\$/dry tonne)		
	Energy usage	Purchase price	Throughput
25% below baseline	\$53.13	\$54.90	\$ 58.24
Baseline	\$55.28	\$55.28	\$ 55.28
25% above Baseline	\$57.43	\$55.64	\$ 52.33

**Table 9**LCA results for torrefaction system compared to wood chips.

Scenario	Torrefied pellet	Wood chip	Notes
Global Warming Potential (in kg CO <sub>2</sub> eq/kg pr	oduct)		
Avoided emissions and biogenic carbon credit	-1.98	-1.83	
Process emissions	0.468	0.053	a
Total per kg product	-1.51	-1.78	
Total on an equivalent functional unit basis (per 31.4 MJ product)	-1.51	-3.43	
Fossil Energy Demand (MJ/kg product)			
Total per kg product	0.73	-1.83	b
Total on an equivalent functional unit basis (per 31.4 MJ product)	0.73 MJ	1.59 MJ	

<sup>&</sup>lt;sup>a</sup> (i) Torrefied pellet: 90% due to torrefaction emissions, 6% electricity, 4% diesel. (ii) Wood chips: 42% collection/processing, 58% transport.

Table 10 LCA scenario analysis results.

,	
Scenario	Global warming potential (kg CO <sub>2</sub> eq/kg product)
Base case: 45% LFG collection efficiency,	-1.512
Composition: 57% Paper, 38% Plastic, 5% Ash	
Lower LFG collection efficiency (30% vs. 45%)	-1.71 (13% decrease)
Higher LFG collection efficiency (60% vs. 45%)	-1.31 (13% increase)

about the prior fate of the MSW. The mix of biogenic vs. fossil components of the MSW, as well as the particular types of biogenic materials in the MSW, will have an impact on the ultimate composition and energy content of the processed pellet, as well as a significant impact on the carbon dynamics within the landfill, which will then impact the process life cycle when avoided landfill emissions are accounted for. Similarly, the climatic conditions of the landfill and the effective management of the landfill in terms of collection of landfill gas and treatment of that gas through flaring or energy generation will impact the landfill emissions that are ultimately avoided when MSW is instead diverted to the torrefaction process. Although a majority of large landfills in the U.S. now have some type of landfill gas collection system, many small landfills exist throughout the U.S. and elsewhere where minimal or no landfill gas collection is performed, and even sound landfill gas collection systems cannot prevent fugitive emissions of methane from occurring over time. As an illustration of these two points, the following scenarios were assessed to understand the GHG emissions impact from even small changes in these key assumptions. The LCA results for these scenarios indicate that both of these assumptions are important. The results appear to be highly sensitive to changing MSW composition for the reasons mentioned above. Additional cases of different MSW compositions will be investigated in future work to verify the processing outcomes of these different MSW streams after torrefaction and to understand the potential differences in their dynamics with a landfill to determine the net effect of MSW diversion.

# 4. Conclusion

Pilot-scale torrefaction technology integrating paddles and extrusion for solid fuel pellet production is presented. This technology resolves biomass-associated challenges like self-heating, difficulty in biomass pelletization, and cost. It also addresses challenges related to the waste fiber-plastic, such as inconsistency, waste-stream heterogeneity, and conveying issues. The produced pellets have low cost, better uniformity, high heating value, and low environmental impact. TEA demonstrates that the baseline cost of pre-processing fiber-plastic wastes is estimated

at \$55.28/dry tonne (2020\$). The crammer-torrefier unit accounts for \$10.08/dry tonne (nearly 42%) of the pre-processing costs. Under a range of scenarios, wherein important parameters are varied, pre-processing costs range between \$52.33/dry tonne and \$58.24/dry tonne. The torrefaction system's life cycle assessment studies illustrate that the pellets can be produced with a net negative global warming potential at this intermediate stage of the life cycle, with a low fossil energy demand relative to a wood chip comparison project. Specific carbon dynamics are highly sensitive to fiber-plastic waste composition and assumptions regarding the prior fate of these materials in the landfill, which will be the subject of future study.

### **Author contribution**

Shreyas S. Kolapkar: Investigation, Methodology, Writing- original draft, review & editing. Stas Zinchik: Investigation, Methodology, Writing- review & editing. Pralhad Burli: Writing- Original technoeconomic analysis section draft. Yingqian Lin: Writing- original technoeconomic analysis section draft. Damon S. Hartley: Writing-original technoeconomic analysis section draft. Jordan Klinger: Writing- Original technoeconomic analysis section draft. Robert Handler: Writing- original life cycle assessment section draft. Ezra BarZiv: Supervision, Investigation, Methodology, Writing- original draft, review & editing.

# Declaration of competing interest

The authors declare no conflict of interest.

# Acknowledgment

We acknowledge support from (1) NSF-PFI Award #1827364, (2) INL Award number #209856, (3) MTRAC Award #RC-109248-MTU-Bar-Ziv-2019. We would like to thank Dr. Armando G. McDonald for the DSC analysis.

### References

- [1] S. Kaza, L.C. Yao, P. Bhada-Tata, F. Van Woerden, What a Waste 2.0: A Global Snapshot of Solid Waste Management to 2050, World Bank, Washington, DC, 2018, https://doi.org/10.1596/978-1-4648-1329-0.
- [2] G. Sauve, K. Van Acker, The environmental impacts of municipal solid waste landfills in Europe: a life cycle assessment of proper reference cases to support decision making, J. Environ. Manag. 261 (2020) 110216, https://doi.org/10.1016/ j.jenyman.2020.110216.
- [3] M.R. Mendes, T. Aramaki, K. Hanaki, Comparison of the environmental impact of incineration and landfilling in São Paulo City as determined by LCA, Resour. Conserv. Recycl. 41 (2004) 47–63, https://doi.org/10.1016/j. rescopres 2003 08 003
- [4] U.S. EPA, Sustainable Materials Management: Non-Hazardous Materials and Waste Management Hierarchy | Sustainable Materials Management | US EPA. htt ps://www.epa.gov/smm/sustainable-materials-management-non-hazardous-materials-and-waste-management-hierarchy, 2020 (accessed September 4, 2021).
- [5] M. Nelles, J. Grünes, G. Morscheck, Waste management in Germany development to a sustainable circular economy? Procedia Environ. Sci. 35 (2016) 6–14, https:// doi.org/10.1016/j.proenv.2016.07.001.
- [6] T.G. Townsend, S. Laux, M. Anshassi, Florida Solid Waste Management: State of the State, Gainesville. https://faculty.eng.ufl.edu/timothy-townsend/wp-content/upl oads/sites/210/2020/06/09\_29\_18\_SOS-Project-HC-Report-Final.pdf, 2018.
- [7] S. of C. Department of Resources and Recovery, State of Disposal and Recycling in California: For Calendar Year 2016. https://www2.calrecycle.ca.gov/Publications
- [8] A.L. Brooks, S. Wang, J.R. Jambeck, The Chinese import ban and its impact on global plastic waste trade, Sci. Adv. 4 (2018), eaat0131, https://doi.org/10.1126/ sciady.aat0131
- [9] Z. Xu, S.S. Kolapkar, S. Zinchik, E. Bar-Ziv, L. Ewurum, A.G. McDonald, J. Klinger, E. Fillerup, K. Schaller, C. Pilgrim, Bypassing energy barriers in fiber-polymer torrefaction, Front. Energy Res. 9 (2021) 1–13, https://doi.org/10.3389/ fenrg.2021.643371.
- [10] Z. Xu, S. Zinchik, S.S. Kolapkar, E. Bar-Ziv, T. Hansen, D. Conn, A.G. McDonald, Properties of torrefied U.S. waste blends, Front. Energy Res. 6 (2018) 1–13, https://doi.org/10.3389/fenrg.2018.00065.

<sup>&</sup>lt;sup>b</sup> (i) Torrefied pellet: 56% electricity, 44% diesel. (ii) Wood chips: 42% collection/processing, 58% transport.

- [11] M.J. Prins, K.J. Ptasinski, F.J.J.G. Janssen, More efficient biomass gasification via torrefaction, Energy. 31 (2006) 3458–3470, https://doi.org/10.1016/j. energy.2006.03.008.
- [12] Q. Chen, J. Zhou, B. Liu, Q. Mei, Z. Luo, Influence of torrefaction pretreatment on biomass gasification technology, Chin. Sci. Bull. 56 (2011) 1449–1456, https://doi. org/10.1007/s11434-010-4292-z.
- [13] Z. Chen, M. Wang, E. Jiang, D. Wang, K. Zhang, Y. Ren, Y. Jiang, Pyrolysis of torrefied biomass, Trends Biotechnol. 36 (2018) 1287–1298, https://doi.org/ 10.1016/j.tibtech.2018.07.005.
- [14] V. Srinivasan, S. Adhikari, S.A. Chattanathan, S. Park, Catalytic pyrolysis of torrefied biomass for hydrocarbons production, Energy Fuel 26 (2012) 7347–7353, https://doi.org/10.1021/ef301469t.
- [15] M.N. Cahyanti, T.R.K.C. Doddapaneni, T. Kikas, Biomass torrefaction: an overview on process parameters, economic and environmental aspects and recent advancements, Bioresour. Technol. 301 (2020) 122737, https://doi.org/10.1016/ ibjortech.2020.122737
- [16] R.W. Nachenius, T.A. van de Wardt, F. Ronsse, W. Prins, Torrefaction of pine in a bench-scale screw conveyor reactor, Biomass Bioenergy 79 (2015) 96–104, https://doi.org/10.1016/j.biombioe.2015.03.027.
- [17] B. Batidzirai, A.P.R. Mignot, W.B. Schakel, H.M. Junginger, A.P.C. Faaij, Biomass torrefaction technology: techno-economic status and future prospects, Energy. 62 (2013) 196–214, https://doi.org/10.1016/j.energy.2013.09.035.
- [18] E.A. Silveira, S. Luz, K. Candelier, L.A. Macedo, P. Rousset, An assessment of biomass torrefaction severity indexes, Fuel. 288 (2021) 119631, https://doi.org/ 10.1016/j.fuel.2020.119631.
- [19] Y. Niu, Y. Lv, Y. Lei, S. Liu, Y. Liang, D. Wang, S. Hui, Biomass torrefaction: properties, applications, challenges, and economy, Renew. Sust. Energ. Rev. 115 (2019) 109395, https://doi.org/10.1016/j.rser.2019.109395.
- [20] J. Koppejan, S. Sokhansanj, S. Melin, S. Madrali, Status Overview of Torrefaction Technologies, IEA Bioenergy, 2015. https://www.ieabioenergy.com/blog/publi cations/status-overview-of-torrefaction-technologies-a-review-of-the-commercialis ation-status-of-biomass-torrefaction/.
- [21] T.R. Brown, A techno-economic review of thermochemical cellulosic biofuel pathways, Bioresour. Technol. 178 (2015) 166–176, https://doi.org/10.1016/j biortech 2014 09 053
- [22] F. Qi, M.M. Wright, Particle scale modeling of heat transfer in granular flows in a double screw reactor, Powder Technol. 335 (2018) 18–34, https://doi.org/ 10.1016/j.powtec.2018.04.068.
- [23] L.J.R. Nunes, A case study about biomass torrefaction on an industrial scale: solutions to problems related to self-heating, difficulties in pelletizing, and excessive wear of production equipment, Appl. Sci. 10 (2020) 2546, https://doi. org/10.3390/app10072546.
- [24] W.H. Chen, B.J. Lin, Y.Y. Lin, Y.S. Chu, A.T. Ubando, P.L. Show, H.C. Ong, J. S. Chang, S.H. Ho, A.B. Culaba, A. Pétrissans, M. Pétrissans, Progress in biomass torrefaction: principles, applications and challenges, Prog. Energy Combust. Sci. 82 (2021). https://doi.org/10.1016/j.pecs.2020.100887.
- [25] S. Zinchik, Z. Xu, S.S. Kolapkar, E. Bar-Ziv, A.G. McDonald, Properties of pellets of torrefied U.S. waste blends, Waste Manag. 104 (2020) 130–138, https://doi.org/ 10.1016/j.wasman.2020.01.009.
- [26] S. Zinchik, Paddle Mixer-Extrusion Reactor for Torrefaction and Pyrolysis, Michigan Technological University, 2019, https://doi.org/10.37099/mtu.dc.etdr/906.
- [27] Z. Xu, S.S. Kolapkar, S. Zinchik, E. Bar-Ziv, J. Klinger, E. Fillerup, K. Schaller, C. Pilgrim, Kinetic study of paper waste thermal degradation, Polym. Degrad. Stab. 191 (2021) 109681, https://doi.org/10.1016/j.polymdegradstab. 2021.109681.
- [28] Z. Xu, J.W. Albrecht, S.S. Kolapkar, S. Zinchik, E. Bar-Ziv, Chlorine removal from U.S. solid waste blends through torrefaction, Appl. Sci. 10 (2020) 1–12, https://doi.org/10.3390/app10093337.
- [29] E. Bar-Ziv, R. Saveliev, M. Perelman, Torrefaction apparatus and process, US 9193916 B2, 2015.
- [30] S. Zinchik, J.L. Klinger, T.L. Westover, Y. Donepudi, S. Hernandez, J.D. Naber, E. Bar-Ziv, Evaluation of fast pyrolysis feedstock conversion with a mixing paddle reactor, Fuel Process. Technol. 171 (2018) 124–132, https://doi.org/10.1016/j. fiuroc.2017.11.012
- [31] S.S. Kolapkar, S. Zinchik, Z. Xu, A.G. McDonald, E. Bar-Ziv, Integration of thermal treatment and extrusion by compounding for processing various wastes for energy applications, Energy Fuel 35 (2021) 12227–12236, https://doi.org/10.1021/acs. energyfuels.101836.
- [32] P.G. Lafleur, B. Vergnes, Polymer Extrusion, John Wiley & Sons, Ltd, Chichester, UK, 2014, https://doi.org/10.1002/9781118827123.
- [33] R.I. Radics, R. Gonzalez, E.M. Bilek, S.S. Kelley, Systematic review of torrefied wood economics, BioResources 12 (2017) 6868–6884, https://doi.org/10.15376/ biores.12.3.6868-6884.

- [34] W. Li, J. Dumortier, H. Dokoohaki, F.E. Miguez, R.C. Brown, D. Laird, M.M. Wright, Regional techno-economic and life-cycle analysis of the pyrolysis-bioenergybiochar platform for carbon-negative energy, Biofuels, Bioprod. Biorefining. 13 (2019) 1428–1438, https://doi.org/10.1002/bbb.2043.
- [35] S. Whalley, S.J.W. Klein, J. Benjamin, Economic analysis of woody biomass supply chain in Maine, Biomass Bioenergy 96 (2017) 38–49, https://doi.org/10.1016/j. biombioe.2016.10.015.
- [36] M.M. Wright, D.E. Daugaard, J.A. Satrio, R.C. Brown, Techno-economic analysis of biomass fast pyrolysis to transportation fuels, Fuel. 89 (2010) S2–S10, https://doi. org/10.1016/j.fuel.2010.07.029.
- [37] S. Boxman, B.F. Stanley, Analysis of MSW Landfill Tipping fees 2020, Environ. Res. Educ. Found. (2021) 1–9. www.erefdn.org.
- [38] G. Vinti, V. Bauza, T. Clasen, K. Medlicott, T. Tudor, C. Zurbrügg, M. Vaccari, Municipal solid waste management and adverse health outcomes: a systematic review, Int. J. Environ. Res. Public Health 18 (2021) 4331, https://doi.org/ 10.3390/ijerph18084331.
- [39] J. Dong, Y. Tang, A. Nzihou, Y. Chi, Key factors influencing the environmental performance of pyrolysis, gasification and incineration Waste-to-Energy technologies, Energy Convers. Manag. 196 (2019) 497–512, https://doi.org/ 10.1016/j.enconman.2019.06.016.
- [40] U.R. Gracida-Alvarez, L.M. Keenan, J.C. Sacramento-Rivero, D.R. Shonnard, Resource and greenhouse gas assessments of the thermochemical conversion of municipal solid waste in Mexico, ACS Sustain. Chem. Eng. 4 (2016) 5972–5978, https://doi.org/10.1021/acssuschemeng.6b01143.
- [41] N.C. Crawford, N. Nagle, D.A. Sievers, J.J. Stickel, The effects of physical and chemical preprocessing on the flowability of corn stover, Biomass Bioenergy 85 (2016) 126–134, https://doi.org/10.1016/j.biombioe.2015.12.015.
- [42] C. Wilèn, P. Jukola, T. Järvinen, K. Sipilä, F. Verhoeff, J. Kiel, Wood torrefaction pilot tests and utilisation, VTT Technol. 122 (2013).
- [43] ASABE, American Society of Agricultural and Biologival Engineers, ASAE D497.5 FEB2006 Standards: Agricultural Machinery Management Data, American Society of Agricultural and Biological Engineers, St. Joseph, MI, 2006.
- [44] AAEA, Commodity Costs and Returns Estimation Handbook, American Agricultural Economics Association, Ames, IA, 2000.
- [45] K.G. Cafferty, D.J. Muth, J.J. Jacobson, K.M. Bryden, Model based biomass system design of feedstock supply systems for bioenergy production, in: Vol. 2B 33rd Comput. Inf. Eng. Conf., American Society of Mechanical Engineers, 2013, https:// doi.org/10.1115/DETC2013-13559.
- [46] Argonne National Laboratory, GREET Life-cycle Model, Center for Transportation Research, Energy System Division, 2019. https://greet.es.anl.gov.
- [47] Engineering Toolbox, Wood and Biomass Heat, Eng. Toolbox. (2003). https://www.engineeringtoolbox.com/wood-biomass-combustion-heat-d\_440.html (accessed June 9, 2021).
- [48] B.P. Weidema, C. Bauer, R. Hischier, C. Mutel, T. Nemecek, J. Reinhard, C. O. Vadenbo, G. Wenet, Data quality guideline for the ecoinvent database version 3. Ecoinvent report 1 (v3), Swiss cent, Life Cycle Invent 3 (2013) 169. http://www.ecoinvent.org/database/methodology-of-ecoinvent-3/methodology-of-ecoinvent-3.html.
- [49] U. S. Environmental Protection Agency, eGRID 2019 Summary Data. https://www.epa.gov/egrid/summary-data, 2021 (accessed June 1, 2021).
- [50] J. Klinger, E. Bar-Ziv, D. Shonnard, Predicting properties of torrefied biomass by intrinsic kinetics, Energy Fuel 29 (2015) 171–176, https://doi.org/10.1021/ ef501456p.
- [51] J. Han, A. Elgowainy, I. Palou-Rivera, J.B. Dunn, M.Q. Wang, Well-to-Wheels Analysis of Fast Pyrolysis Pathways with GREET, Oak Ridge, TN. https://publications.anl.gov/anlpubs/2011/12/71546.pdf, 2011.
- [52] Y. Lu, W. Jin, J. Klinger, T.L. Westover, S. Dai, Flow characterization of compressible biomass particles using multiscale experiments and a hypoplastic model, Powder Technol. 383 (2021) 396–409, https://doi.org/10.1016/j. powter 2021 01 027
- [53] Y. Xia, J.J. Stickel, W. Jin, J. Klinger, A review of computational models for the flow of milled biomass part I: discrete-particle models, ACS Sustain. Chem. Eng. 8 (2020) 6142–6156, https://doi.org/10.1021/acssuschemeng.0c00402.
- [54] W. Jin, J.J. Stickel, Y. Xia, J. Klinger, A review of computational models for the flow of milled biomass part II: continuum-mechanics models, ACS Sustain. Chem. Eng. 8 (2020) 6157–6172, https://doi.org/10.1021/acssuschemeng.0c00412.
- 55] J. Mody, R. Saveliev, E. Bar-Ziv, M. Perelman, Production and characterization of biocoal for coal-fired boilers, in: Vol. 1 Fuels Combust. Mater. Handl. Emiss. Steam Gener. Heat Exch. Cool. Syst. Turbines, Gener. Aux. Plant Oper. Maintenance; Reliab. Availab. Maintainab. (RAM); Plant Syst., American Society of Mechanical Engineers, 2014, https://doi.org/10.1115/POWER2014-32036.
- [56] D. Abbas, R.M. Handler, Life-cycle assessment of forest harvesting and transportation operations in Tennessee, J. Clean. Prod. 176 (2018) 512–520, https://doi.org/10.1016/j.jclepro.2017.11.238.